Effects of Temperature and Suction on Plastic Deformation of Unsaturated Soil under Cyclic Loads

Type of paper: General paper

Authors: C. Zhou*and C. W. W. Ng

*Corresponding author

Information of the authors

First author: Dr C. Zhou

Visiting assistant professor, Department of Civil and Environmental Engineering, The Hong Kong University of Science and Technology, Clear Water Bay, Kowloon, Hong Kong.

E-mail: czhou@connect.ust.hk

Co-author: Dr C. W. W. Ng

Chair professor, Department of Civil and Environmental Engineering, The Hong Kong University of Science and Technology, Clear Water Bay, Kowloon, Hong Kong.

E-mail: cecwwng@ust.hk

Abstract

Subgrade soils are usually unsaturated and subjected to daily variation of temperature and suction (water content) in the field. Their plastic deformation may accumulate under cyclic traffic loads and induce cracking and rutting in the asphalt and concrete layers of a pavement. So far, thermal and suction effects on the accumulation of plastic strain have not been fully understood. In this study, cyclic triaxial tests on unsaturated subgrade soil were carried out using a temperature- and suction-controlled triaxial system. Temperatures from 20 to 60℃ and suctions from 0 to 60 kPa were considered. Experimental results reveal that at the same cyclic load, the measured plastic strain of soil is significantly larger at lower suction and higher temperature. This is likely because the yield stress of unsaturated soil increases with increasing suction (suction hardening), but decreases with increasing temperature (thermal softening). With a higher yield stress, the same cyclic load would induce smaller plastic strain. Moreover, these observations imply that current pavement design methods, which determine soil parameters at room temperature and ignore thermal effects, would underestimate soil deformation induced by cyclic traffic loads when in-situ temperature is significantly higher than room temperature.

Keywords

Subgrade soil, cyclic, plastic strain accumulation, unsaturated, suction, temperature

Introduction

It is well recognized that cyclic traffic loads would induce plastic deformation of subgrade soil in a pavement (Lekarp et al., 2000; Puppala et al., 1999; Mishra and Tutumluer, 2012). Furthermore, the plastic deformation would accumulate with increasing number of cycles and affect the long-term performance of a pavement significantly (Lekarp et al., 2000). Any non-uniform deformation may induce cracking and rutting in the asphalt and concrete layers of a pavement (Brown, 1996; Lekarp et al., 2000; Ng and Zhou, 2014). On the other hand, subgrade soil in the field is often unsaturated and subjected to daily variations of suction (water content) and temperature (Jin et al., 1994; Amiri et al., 2009; McCartney and Khosravi, 2013). Many theoretical and experimental studies have revealed that unsaturated soil behaviour is highly dependent on suction and temperature (e.g., Romero et al., 2003; Zhou et al., 2014). Most of these studies, however, focused on soil behaviour under monotonic loading. To enhance the design of a pavement, it is essential to understand suction and thermal effects on plastic strain accumulation of unsaturated subgrade soil under cyclic loads.

To investigate the influence of soil moisture on plastic strain accumulation, some researchers compacted soil specimen at different water contents and then measured plastic strain accumulation characteristics of each specimen through cyclic triaxial tests (e.g., Sivakumar et al., 2013). It was found that at the same stress condition, plastic strain accumulated under cyclic loads decreases with a decrease in water content (i.e., an increase in suction). This approach has certain limitations: different compaction water contents could induce differences in both suction and inherent soil structure (Alonso et al., 2013). It is difficult to separate the effects of suction from the effects of soil structure. To tackle this problem, suction-controlled tests should be carried out using specimens prepared at the same initial water content.

As far as thermal effects on plastic strain accumulation are concerned, Ng and Zhou (2014) carried out a series of temperature- and suction-controlled cyclic triaxial tests on unsaturated compacted silt. Based on limited data, they observed that the plastic strain, which accumulates under cyclic loading and unloading, increases with increasing temperature but decreasing suction. It should be noted that the principal objective of Ng and Zhou was to study thermal and suction effects on resilient modulus of unsaturated subgrade soil. The accumulation of plastic strain was not analysed in detail. Some important aspects, for example, effects of heating and cooling, cyclic stress and number of cycles on plastic strain accumulation, were not investigated.

The current paper is a continuation and extension of the research work reported by Ng and Zhou (2014). The data of Ng and Zhou was reinterpreted with a focus on the plastic strain accumulation of unsaturated soil induced by cyclic loads. Furthermore, to supplement the existing data, more cyclic triaxial tests were carried out using a temperature- and suction-controlled triaxial system developed by Ng and Zhou. The influences of number of cycles, suction, temperature and number of cycles on plastic strain accumulation of subgrade soil under cyclic loads were analysed in detail. The measured and interpreted results would be useful for predicting irreversible settlement of subgrade soils and hence the performance of a pavement.

TEST PROGRAM AND APPARATUS

Two series of temperature- and suction-controlled cyclic triaxial tests were carried out in this study. The principal objective of the first series of tests was to investigate thermal and suction effects on cyclic behaviour of unsaturated soil. Nine triaxial tests (W0T20, W0T40, W0T60, W30T20, W30T40, W30T60, W60T20, W60T40 and W60T60) were conducted in this series of tests. Three suctions (0, 30 and 60 kPa) were used. At each suction level, three tests were carried out at different temperatures (20, 40 and 60℃). The second series of tests were designed to study the influence of heating and cooling on cyclic behaviour of unsaturated subgrade soil. In this series, two tests (W30HC and W60HC) were carried out at 20℃ and at suctions of 30 and 60 kPa. Different from the tests in the first series, W30HC and W60HC were subjected to a cycle of heating and cooling prior to the application of cyclic loads. By comparing the responses between W30T20 and W30HC, the influence of heating and cooling at suction of 30 kPa was analysed. Similarly, the results of W60T20 and W60HC were compared to study effects of heating and cooling at suction of 60 kPa. Details of the test program are given in Table 1. It should be pointed out that W30T60, W60T60, W30HC, W60HC are the new tests compared to Ng and Zhou (2014).

Figure 1 shows the schematic diagram of a temperature and suction-controlled triaxial apparatus for testing cyclic behaviour of subgrade soil at various suctions and temperatures (Ng and Zhou, 2014). Matric suction (u_a-u_w), where u_a and u_w are pore air pressure and pore water pressure respectively, was controlled using the axis-translation technique. This technique imposes u_a-u_w on the soil specimen by controlling u_a and u_w independently. u_a was controlled through a coarse, low air-entry value (AEV) porous stone sitting on top of the soil specimen. u_w was controlled through a saturated, high AEV (i.e., 3 bar) ceramic disc sealed to the pedestal of the triaxial cell. The saturated ceramic disc permitted the exchange of water through it but prevented the passage of free air as long as u_a-u_w was lower than its AEV. However, dissolved air in water may pass through the ceramic disc and accumulate either underneath the ceramic disc or in the water drainage system. In this study, any accumulated air bubble was flushed out and collected once every 24 h using a diffused air volume indicator (Fredlund, 1975). The volume of collected air was used to correct the measured change in soil water content.

To control soil temperature, a heating system consisting of thermostat, heater and thermocouples was added to the apparatus. As shown in the figure, the heater and thermocouple A were installed inside the triaxial cell. Both of them were connected to the thermostat, forming a closed-loop control and feedback system. During testing, the thermostat adjusted the heater output based on feedback from thermocouple A. When the dissipating energy and the heater output were balanced, the air temperature inside the triaxial cell reached equilibrium. It is reasonable to assume that the soil temperature is equal to the air temperature in the triaxial cell at equilibrium state. To enhance the uniformity of temperature inside the triaxial cell, two small fans and a hollow aluminium cylinder were installed in the triaxial cell. The fan improved air circulation, while the aluminium cylinder enhances heat transfer because of its high thermal conductivity. To check the uniformity of temperature, two thermocouples (A and B) were installed at different locations inside the triaxial cell. They measured air temperature at a distance of about 5 mm from the soil specimen. When thermal equalisation was reached, readings of the two thermocouples were almost identical. They remained fairly constant with a maximum fluctuation of ±0.5℃.

In addition to the conventional external measurement of axial strain using a linear variable differential transformer (LVDT), the cyclic triaxial system was equipped with three Hall effect transducers (Clayton et al., 1989). As shown in Figure 1, the Hall effect transducers measured local soil deformation at the mid-height of each specimen. One of these Hall effect transducers was used to measure radial deformation, while the other two were used to measure axial deformation independently. After calibration, the resolution and accuracy of each Hall effect transducer were about 1 and 3 μm respectively, corresponding to vertical strains of about 0.001% and 0.003% (Ng and Xu, 2012). As expected, axial strain obtained using an LVDT (external device) was generally larger than that obtained using a Hall effect transducer (local device). This is because the former method measures the overall deformation of a soil specimen together with bedding errors and compliance of the system (Jardine et al., 1984), whereas the latter records the actual displacement of the soil specimen. For greater reliability, axial strain measured using Hall effect transducers was used and reported.

Since the Hall effect transducers measured local deformation at the mid-height of a specimen, it was sensible to measure pore water pressure also at this level. A suction probe was employed to monitor pore water pressure at the mid-height of a specimen during cyclic loading-unloading, although a conventional pore water pressure transducer was still used to measure pore water pressure at the bottom. For unsaturated soil testing, pore water pressure measured at the mid-height also provides guidance for suction equalisation. The suction probe was modified from a Druck PDCR-81 miniature pore water pressure transducer by replacing the low AEV ceramic tip with a high AEV ceramic tip (500 kPa) (Ng and Xu, 2012). Thus it was able to measure negative pore water pressure of up to 480 kPa, close to the AEV of the ceramic tip.

Considering that the Hall effect transducers and the suction probe were exposed to elevated temperatures, they were carefully calibrated in a temperature-controlled oven at three temperatures (20, 40 and 60°C). At each temperature, they were calibrated under both loading and unloading conditions. The experimental results reveal that both suction probe and Hall effect transducer are sufficiently temperature compensated in the temperature range from 20 to 60°C. The thermal insensitivity of these transducers ensures accurate measurement of pore water pressure and soil deformation at various temperatures. More details of calibration results were reported by Ng and Zhou (2014).

SOIL TYPE AND SPECIMEN PREPARATION

The material investigated in this study is a completely decomposed tuff (CDT) sampled from Hong Kong. It is yellowish-brown, slightly plastic and contains very small percentages of fine sand and coarse sand. Figure 2(a) shows the particle size distribution as determined by sieve and hydrometer analyses (BSI, 1990). In addition, the physical properties are summarised in Table 2. According to the Unified Soil Classification System, CDT is classified as silt (ML) (ASTM, 2006).

Previous studies have shown that the mechanical and hydraulic behaviours of unsaturated soils are fully coupled (e.g., Wheeler et al., 2003). To study the hydraulic behaviour of CDT, water retention curve of compacted CDT was measured using a triaxial pressure plate system (Ng et al., 2013). Figure 2(b) shows the measured drying and wetting curves. The figure reveals that along the drying path, volumetric water content decreases non-linearly as suction increases. The AEV is estimated to be 60 kPa. Along the wetting path, the adsorption rate changes abruptly at a suction of about 30 kPa. Although the water retention curve was measured only at 20°C, thermal effects on the curve may be estimated based on previous experimental studies, where it has been found that the water retention capacity of unsaturated soil reduces slightly with an increase in temperature (Romero et al., 2001).

Each specimen, 76 mm in diameter and 152 mm in height, was statically compacted in 10 layers in the current study. The compaction water content was 16.3±0.1%, with an average value corresponding to the optimum water content as determined in the Standard Proctor Compaction test (BSI, 1990). To minimize excessive compaction of the lower layers during compaction of the upper layers, the process of compaction was stress-controlled with a maximum compaction pressure of 1200 kPa. After sample compaction, the initial dry density of each soil specimen was found to be about 1.73±0.02 g/cm^3, which corresponds to a dry density ratio of 98±1%. The height and diameter of the specimen were measured by a calliper (readable to 0.01 mm) and a PI tape (readable to 0.01 mm), respectively. The average initial suction of the specimens after compaction was 95 kPa as measured the suction probe shown in Figure 1. The variations in measured initial suction at different heights of each specimen and among different specimens were all less than ±2 kPa.

Ng and Yung (2008) carried out a series of isotropic compression tests on compacted CDT specimens. The initial dry density of soil specimens in their study is 1.68 g/cm^3, which is about 3% smaller than that used in the current test program. The compaction water contents in both studies are 16.3%. Considering that these two studies adopt very close initial density and water content, experimental results reported by Ng and Yung are used to assist the interpretations of current data. At suctions of 0, 50 and 100 kPa, the yield stresses of compacted specimens were found to be about 120, 170 and 200 kPa, respectively. Based on these results, the loading collapse (LC) curve at 20℃ was determined and is shown in Figure 2(c). It can be seen that yield stress increases with increasing suction (suction hardening). In addition, an isotropic compression test was carried out at zero suction and 40℃ in this study. The corresponding yield stress was about 105 kPa. Assuming that the shape of the LC curve is independent of temperature, the LC curve at 40℃ was deduced and is also shown in the figure. It is revealed that yield stress decreases with an increase in temperature at a given suction (thermal softening).

TEST PROCEDURES

In this study, there are four stages in each temperature- and suction-controlled cyclic triaxial test, including isotropic compression, suction equalisation, thermal equalisation and cyclic loading-unloading. Figure 3 shows the thermo-hydro-mechanical path of each specimen in the first three stages. After compaction, each specimen was set up in the triaxial system. The initial stress state of each specimen was controlled at point A. Each specimen was firstly isotropically compressed to a net confining stress of 30 kPa at constant water content (A→B).

According to AASHTO (2003) standard for resilient modulus tests on subgrade soil, the confining pressure applied should be in the range from 2 to 6 psi (13.8 to 41.4 kPa). A single pressure of 30 kPa, which is close to the mean value (4 psi), was therefore considered and adopted. It should be pointed out that effects of net confining pressure on cyclic behaviour were not investigated in this study. This is because they are widely investigated in previous studies (e.g., Sivakumar et al., 2013). It should be noted that there is no standard methods for measuring plastic strain accumulation of subgrade soil, the AASHTO standard for testing resilient modulus of subgrade soil through cyclic triaxial tests was thus considered and used.

After isotropic compression, soil specimen was wetted by decreasing suction from 95 kPa to 0, 30 and 60 kPa (B→E, B→D and B→C). To control soil suction, predefined u_a and u_w were applied from the top and bottom, respectively. Then the soil specimen was subjected to suction equalisation. The equalisation was considered to be completed when the water flow of the soil specimen was less than 0.5 cm^3 within 24 h, corresponding to a rate of water content change of less than 0.04% per day (Sivakumar, 1993). After suction equalisation, suction throughout the soil specimen was equal to the difference between u_a and u_w.

The third stage of each test was thermal equalisation. For three tests carried out at room temperature (20℃) (W0T20, W30T20, W60T20), soil temperature remained constant. For the six tests carried out at elevated temperatures, three specimens (W0T40, W30T40 and W60T40) were heated to 40℃ (E→E_1, D→D_1, and C→C_1), while the other three specimens (W0T60, W30T60 and W60T60) were heated to 60℃ (E→E_2, D→D_2, and C→C_2). Furthermore, the two specimens in tests W30HC and W60HC were heated to 60℃ and then cooled to 20℃

($D \rightarrow D_2 \rightarrow D$ and $C \rightarrow C_2 \rightarrow C$). It should be noted that thermal loading may induce excess pore water pressure. In this study, 3-5 days were needed for the dissipation of excess pore water pressure, depending on suction and temperature conditions. With such a long duration, it was sufficient for each soil specimen to reach the predefined temperature and suction conditions. It should be pointed out that the volume change induced by wetting and heating was quite small (less than 0.1%). This is because in the suction and temperature range considered, the yield stress of soil specimen is larger than 100 kPa (see Figure 2(c)) which is much larger than the net confining pressure of 30 kPa. Therefore, soil response is essentially elastic and the volume change is small.

After equalisation of both suction and temperature, cyclic loads were applied to each specimen to investigate plastic soil deformation under cyclic loads. Cyclic deviator stress in haversine form was applied, while net confining pressure was maintained constant at 30 kPa. At each suction and temperature condition, 100 cycles were applied at a frequency of 1 Hz. The difference between maximum and minimum applied deviator stresses is defined as cyclic stress q_{cyc}. With references to AASHTO (2003) standard for resilient modulus tests, four levels of cyclic stress (30, 40, 55 and 70 kPa) were applied to each specimen in succession. The origin of shear and volumetric strains (i.e., $\varepsilon_q = 0$ and $\varepsilon_v = 0$) is taken after suction and thermal equalisation but before applying the first level of cyclic stress.

During cyclic loading-unloading, the condition of constant water content was simulated for subgrade soil because the dissipation rate of excess pore water pressure was relatively low compared to the rate of repeated traffic loads in the field. In each test, the drainage valve for water was closed and pore water pressure was measured at the base and mid-height of soil specimen. Previous researchers found that pore water pressure measurement at the mid-height is more representative, since it is not affected by end restraint (Hight, 1982). Based on the measurement at mid-height, in all the tests shown in Table 1, the excess pore water pressure is always less than 5 kPa. The relatively small variations in pore water pressure suggest that changes in suction under cyclic loading-unloading may be negligible in this study.

INTERPRETATIONS OF EXPERIMENTAL RESULTS

Influence of number of cycles on plastic strain accumulation

Figure 4(a) shows the stress- strain relationship of unsaturated subgrade soil measured during a typical 100-cycle triaxial test (test W0T20). For clarity, only the first and last 10 cycles are shown in the figure. During the first 10 cycles, axial plastic strain accumulates with increasing number of cycles (*N*). The axial plastic strain induced by the first cycle is much larger than each incremental axial plastic strain induced by any subsequent cycle. During the last 10 cycles, there is no obvious additional accumulation of axial plastic strain, implying that the soil specimen has reached a stable resilient response. For the test shown in the figure, axial plastic strain induced by 100 cycles ($\varepsilon_{ap(100)}$) is equal to about 0.22%.

Figure 4(b) shows the volumetric strain measured during cyclic loading and unloading in test W0T20. It can be seen that during the first 10 cycles, contractive volumetric strain accumulates as *N* increases. During the last 10 cycles, the soil response becomes almost reversible. This is consistent with the measurement of axial strain, as shown in Figure 4(a). The contractive volume change during cyclic loading-unloading induces soil densification and strain hardening. According to the theory of elastoplasticity (Alonso et al., 1990), preconsolidation pressure of soil specimen would increase due to the occurrence of strain hardening. The LC curve shown in Figure 2(c) would shift to the right. Lackenby et al. (2007) carried out a series of cyclic triaxial tests on dry sand. They found that the accumulation of axial plastic strain is not obvious after 10,000 cycles, while volumetric plastic strain accumulates continuously even after 1,000,000 cycles. Compared to previous studies, the number of cycles required to reach a stable response (plastic shakedown) in this study is much smaller. This may be because the CDT specimens in this study were overconsolidated to a large extent.

To further analyse the typical soil response, the accumulation of axial plastic strain with number of cycles (*N*) in test W0T20 is shown in Figure 5(a). Axial plastic strain accumulates continuously with increasing number of cycles, but at different rates. As expected, at the same number of cycles, the accumulated plastic strain is consistently higher at a larger cyclic stress. The accumulation of axial plastic strain under cyclic loads has been extensively studied by previous researchers (Brown, 1996; Lekarp et al., 2000). Some semi-empirical equations are proposed to describe the relationship between axial plastic strain and number of cycles. One of the most widely used formulations adopts a power function (Sweere, 1990):

$$\varepsilon_{ap(N)} = AN^{b} \tag{1}$$

where ε_{ap} is accumulated plastic strain; N is the number of cycles; A and b are soil parameters. According to this equation, parameter A should be equal to plastic strain induced by the first cycle (i.e., $\varepsilon_{ap(1)}$). Parameter b is always assumed to be a constant value in previous studies (e.g., Li and Selig, 1996). To evaluate this assumption, $\varepsilon_{ap(N)}$ is normalized using $\varepsilon_{ap(1)}$. The relationship between $\varepsilon_{ap(N)}/\varepsilon_{ap(1)}$ and N is shown in Figure 5(b). It is clearly revealed that the relationship between $\varepsilon_{ap(N)}/\varepsilon_{ap(1)}$ and N is dependent on cyclic stress. At cyclic stresses of 30 and 40 kPa, the relationship is almost identical. Total increase in $\varepsilon_{ap(N)}/\varepsilon_{ap(1)}$ during the 100 cycles is about 40%. At cyclic stresses of 55 and 70 kPa, the total increase during 100 cycles is about 60% and 100%, respectively. This observation suggests that parameter b in equation (1) is independent of cyclic stress at low cyclic stress, but increases with increasing cyclic stress at high cyclic stress. More discussion of the influence of cyclic stress is given later.

In this study, 100-cycle tests were carried out at various conditions of stress, suction and temperature. At different test conditions, the accumulation of plastic strains with increasing number of cycles follows a qualitatively similar trend. The influence of number of cycles on plastic strain accumulation is not the focus of the current study. To keep the text clear yet concise, the relationship between plastic strain and number of cycles at other test conditions are not presented here. In the following sections, experimental results of $\varepsilon_{ap(100)}$ are presented with a focus on the influence of temperature, suction, cyclic stress and heating and cooling.

Influence of temperature on plastic strain accumulation

Figure 6 shows the influence of temperature on $\varepsilon_{ap(100)}$ at three different suctions (0, 30 and 60 kPa), obtained from Series 1 tests. It is clear that thermal effects on $\varepsilon_{ap(100)}$ are qualitatively similar at different suctions. At a given suction, $\varepsilon_{ap(100)}$ increases consistently with an increase in temperature. Cekerevac and Laloui (2010) carried out a series of temperature-controlled cyclic triaxial tests on saturated reconstituted Kaolin clay at normally consolidated state. They observed that cyclic loading-unloading on the heated sample induced a smaller axial strain per cycle than cyclic loading-unloading on the unheated sample. The seemingly contradictory results from their study and the present one may be attributed to the fact that the soil specimens in the two studies were heated at different overconsolidation ratios (OCRs). According to thermo-hydro-mechanical constitutive models (e.g., François and Laloui, 2008), yield stress decreases with an increase in temperature. For overconsolidated soil (CDT in this study), the yield stress is beyond 100 kPa (see Figure 2(c)) which is much larger than the net confining stress of 30 kPa. It is therefore that soil stress state was inside yield surface during the heating process. Apparent overconsolidation ratio decreased as temperature increased (thermal softening). Given a smaller overconsolidation ratio, larger axial plastic strain developed in the heated specimen during the subsequent stage of cyclic loading-unloading. For normally consolidated soil, soil stress state lies on the yield surface. Heating soil specimen at drained condition does not alter the preconsolidation pressure and OCR. This is because effects of thermal softening could be compensated by effects of strain hardening. Cekerevac and Laloui (2010) measured contractive volumetric strains of up to 1% when normally consolidated Kaolin clay was heated from 22 to 90℃. Thermal loads densified the soil specimen. At the subsequent stage of cyclic loading- unloading, a smaller $\varepsilon_{ap(100)}$ was induced on the heated specimen than on the unheated specimen.

The observations in this figure imply that at a higher in-situ temperature, plastic strain of heavily compacted subgrade soil induced by the same cyclic traffic loads could be larger. As far as the authors are aware, however, current pavement design methods do not consider thermal effects on soil behaviour since soil specimen is only required to be tested at room temperature (Highways-Agency, 2006; AASHTO, 2008). When the in-situ temperature is significantly higher than room temperature, ignoring thermal effects may underestimate soil deformation induced by cyclic traffic loads. Pavement designs, which use soil parameters determined at room temperature, can be therefore unconservative.

Influence of suction on plastic strain accumulation

Figure 7(a) shows the relationship between $\varepsilon_{ap(100)}$ and soil suction at 20℃, obtained from Series 1 tests. At each level of cyclic stress, $\varepsilon_{ap(100)}$ decreases nonlinearly with an increases in suction. The decrease in $\varepsilon_{ap(100)}$ with an increase in suction is probably because as suction increases, the yield stress of soil specimen increases, as shown in Figure 2(c). Given a larger yield stress and OCR, soil specimen behaves stiffer.

Figure 7(b) and Figure 7(c) shows the influence of soil suction on $\varepsilon_{ap(100)}$ at 40 and 60℃, respectively. At different temperatures, $\varepsilon_{ap(100)}$ decreases with an increase in s following a similar trend. At a quantitative level, when cyclic stress is 70 kPa, the accumulated $\varepsilon_{ap(100)}$ decreases from about 2% to 0.5% as suction increases from 0 to 60 kPa (see Figure 7(a)). The total reduction is about 1.5%. At cyclic stress of 70 kPa and temperature of 40 and 60℃, the total reductions of $\varepsilon_{ap(100)}$ are about 2% and 2.5% (see Figure 7(b) and Figure 7(c)). The reduction of $\varepsilon_{ap(100)}$ with an increase in suction seems more significant at higher temperature. This may be because the OCR of heated specimen is smaller than that of unheated specimen due to thermal softening, as illustrated in Figure 2(c). It is therefore that the plastic deformation of heated specimen induced by cyclic loads is lager and differences induced by suction are also more obvious.

Some current design guides have considered effects of soil moisture on soil behaviour using empirical methods. For example, AASHTO (2008) for pavement design suggests that soil specimen is prepared and tested at a reference moisture condition at or near optimum water content. Variations in soil behaviour with soil moisture are then estimated using some empirical models. Since suction effects on soil behaviour depend on temperature, as illustrated in Figure 7, regression parameters in these empirical models should be a function of temperature. To incorporate coupled suction effects on soil behaviour in pavement design, suction and temperature controlled cyclic tests are recommended for calibrating the empirical models.

Influence of cyclic stress on plastic strain accumulation

Figure 8(a) shows the relationship between $\varepsilon_{ap(100)}$ and cyclic stress (q_{cyc}) at various suctions and at 20℃, obtained from Series 1 tests. As expected, measured $\varepsilon_{ap(100)}$ increases with an increase in q_{cyc} at all suctions, but at different rates. Based on a series of cyclic triaxial tests on unsaturated compacted fine-grained soil, Brown (1996) found that there is a threshold q_{cyc} above which accumulation of $\varepsilon_{ap(100)}$ becomes much more significant. For the CDT tested in this study, at zero suction, $\varepsilon_{ap(100)}$ increases non-linearly with an increase in q_{cyc} at an increasing rate. The threshold q_{cyc} is estimated to be between 40 and 55 kPa. It should be noted that the threshold q_{cyc} identified from this figure is closely related to the relationship between $\varepsilon_{ap(N)}/\varepsilon_{ap(1)}$ and N shown in Figure 5(b). When cyclic stress is smaller than threshold value (q_{cyc} = 30 and 40 kPa), the relationship between $\varepsilon_{ap(N)}/\varepsilon_{ap(1)}$ and N is almost identical

(40%) and hence parameter b in equation (1) is constant. When cyclic stress is larger than threshold value (q_{cyc} = 55 and 70 kPa), the total increase during 100 cycles is about 60% and 100% respectively and hence parameter b in equation (1) increases with an increase in q_{cyc}.

On the other hand, Figure 8(a) reveals that the relationship between $\varepsilon_{ap(100)}$ and q_{cyc} is almost linear at suctions of 30 and 60 kPa. It is reasonable to conclude that the threshold q_{cyc} at these two suctions should be larger than 70 kPa. The increase of threshold q_{cyc} with suction is likely due to suction hardening. As shown in Figure 2(c), yield stress increases as suction increases. Given a larger yield stress, a larger q_{cyc} is required to induce significant accumulation of axial plastic strain.

Figure 8(b) and Figure 8(c) shows the relationship between $\varepsilon_{ap(100)}$ and q_{cyc} at 40 and 60℃, respectively. The influence of q_{cyc} on $\varepsilon_{ap(100)}$ at these two temperatures is quite similar to that observed at 20℃ (see Figure 8(a)). Comparisons between these three figures reveal that only at suction of 30 kPa, thermal effects on the threshold q_{cyc} can be identified. At this suction level, the threshold q_{cyc} is found to be larger than 70 kPa at 20 and 40℃ but it is in the range of 40 and 55 kPa at 60℃. This observed decrease in q_{cyc} with increasing temperature is likely because when soil temperature increases, the yield stress and hence the threshold q_{cyc} decreases (see Figure 2(c)). It should be noted that thermal effects on the threshold q_{cyc} are not as obvious as suction effects. Thermal effects at suctions of 0 and 60 kPa cannot be clearly identified based on the limited data.

Influence of heating and cooling on plastic strain accumulation

Figure 9 shows the influence of heating and cooling on M_R at suctions of 30 and 60 kPa, obtained from Series 2 tests. At both suctions (30 and 60 kPa), the same cyclic loads induce smaller $\varepsilon_{ap(100)}$ on soil specimens which have experienced a heating and cooling cycle. The effects of heating and cooling on plastic strain accumulation may be explained by the findings of Abuel-Naga et al. (2007), who carried out a temperature-controlled oedometer test to investigate effects of thermal cycle on the preconsolidation pressure of saturated reconstituted Bangkok clay. In their test, a normally consolidated specimen was heated from 20 to 90℃ and then cooled to 20℃ at drained condition. The heating and cooling cycles induced a contractive volumetric strain. During the subsequent compression process, soil specimen subjected to a heating and cooling cycle was found to behave stiffer. In the current study, compacted CDT specimens are overconsolidated. Although contractive volumetric strain induced by heating and cooling cycle is smaller, the heating and cooling cycle would still slightly stiffen soil specimen.

Conclusions

During cyclic loading and unloading, plastic strain of unsaturated subgrade soil accumulates with increasing number of cycles at a decreasing rate. Each unsaturated specimen tested almost reaches a stable reversible response (plastic shakedown) within 100 cycles. The number of cycles required to achieve a stable response is much smaller than that for dry sand. This is likely attributed to the effects of high OCR and suction hardening of the unsaturated specimen.

At the same cyclic stress, the measured plastic strain is significantly larger at lower suction and higher temperature. Effects of suction and temperature are likely because yield stress of unsaturated subgrade soil increases with increasing suction (suction hardening), but decreases with increasing temperature (thermal softening). With a higher yield stress, smaller plastic strain would be induced by cyclic loading and unloading.

The plastic strain induced by cyclic loads increases significantly with an increase in cyclic stress. There is a threshold cyclic stress above which the accumulation of plastic strain becomes much more significant. The threshold cyclic stress increases with an increase in suction and a decrease in temperature. Compared to suction effects, thermal effects on the threshold cyclic stress is much less significant.

At the same suction, temperature and stress condition, cyclic loads induce smaller plastic strain on soil specimens that have been subjected to a heating and cooling cycle. This may be because heating process induces irreversible contractive soil deformation and therefore stabilize soil skeleton.

It is evident that the plastic strain accumulation of unsaturated subgrade soil is affected by temperature. Since current pavement design methods do not normally consider thermal effects on soil behaviour, soil deformation induced by cyclic traffic loads may be underestimated when in-situ temperature is significantly higher than room temperature.

Acknowledgements

The research grant 2012CB719805 of 2012CB719800 provided by the Ministry of Science and Technology of the People's Republic of China through the National Basic Research Program (973 project) is gratefully acknowledged. In addition, the authors would like to thank the Research Grants Council of the Hong Kong Special Administrative Region (HKSAR) for financial support through research grant HKUST6/CRF/12R.

References

AASHTO (2003). Standard method of test for determining the resilient modulus of soils and aggregate materials. *American Association of State Highway and State Highway Officials, Washington, D.C.*

AASHTO (2008). Mechanical empirical pavement design guide: a manual of practice. *American Association of State and Highway Transportation Officials, Washington D.C.*

Abuel-Naga, H., Bergado, D., Bouazza, A. & Ramana, G. (2007). Volume change behaviour of saturated clays under drained heating conditions: experimental results and constitutive modeling. *Canadian Geotechnical Journal*, 44(8): 942-956.

Alonso, E. E., Gens, A. & Josa, A. (1990). A constitutive model for partially saturated soils. *Géotechnique*, 40(3): 405-430.

Alonso, E. E., Pinyol, N. M. & Gens, A. (2013). Compacted soil behaviour: initial state, structure and constitutive modelling. *Géotechnique*, 63(6): 463-478.

Amiri, H., Nazarian, S. & Fernando, E. (2009). Investigation of impact of moisture variation on response of pavements through small-scale models. *Journal of Materials in Civil Engineering, ASCE*, 21(10): 553-560.

ASTM (2006). *Standard practice for classification of soils for engineering purposes (unified soil classification system)*, American Society of Testing and Materials, West Conshohocken.

Brown, S. F. (1996). Soil mechanics in pavement engineering. *Géotechnique*, 46(3): 383-425.

BSI (1990). *Methods of test for soils for civil engineering purposes*, British Standards Institution, London.

Cekerevac, C. & Laloui, L. (2010). Experimental analysis of the cyclic behaviour of kaolin at high temperature. *Géotechnique*, 60(8): 651-655.

Clayton, C., Khatrush, S., Bica, A. & Siddique, A. (1989). Hall effect sensors in geotechnical instrumentation. *Geotechnical Testing Journal*, 12(1): 69-76.

François, B. & Laloui, L. (2008). ACMEG-TS: A constitutive model for unsaturated soils under non-isothermal conditions. *International Journal for Numerical and Analytical Methods in Geomechanics*, 32(16): 1955-1988.

Fredlund, D. G. (1975). Diffused air volume indicator for unsaturated soils. *Canadian Geotechnical Journal*, 12(4): 533-539.

Hight, D. (1982). A simple piezometer probe for the routine measurement of pore pressure in triaxial tests on saturated soils. *Géotechnique*, 32(4): 396-401.

Highways-Agency (2006). *Design manual for roads and bridges, vol. 7*, The Stationery Office, London, UK.

Jardine, R. J., Symes, M. J. & Burland, J. B. (1984). The Measurement of Soil Stiffness in the Triaxial Apparatus. *Géotechnique*, 34(3): 323-340.

Jin, M. S., Lee, K. W. & Kovacs, W. D. (1994). Seasonal variation of resilient modulus of subgrade soils. *Journal of Transportation Engineering*, 120(4): 603-616.

Lackenby, J., Indraratna, B., McDowell, G. & Christie, D. (2007). Effect of confining pressure on ballast degradation and deformation under cyclic triaxial loading. *Géotechnique*, 57(6): 527-536.

Lekarp, F., Isacsson, U. & Dawson, A. (2000). State of the art. II: Permanent strain response of unbound aggregates. *Journal of Transportation Engineering*, 126(1): 76-83.

Li, D. & Selig, E. T. (1996). Cumulative plastic deformation for fine-grained subgrade soils. *Journal of Geotechnical Engineering, ASCE*, 122(12): 1006-1013.

Lopez-Querol, S. & Coop, M. R. (2012). Drained cyclic behaviour of loose Dogs Bay sand. *Géotechnique*, 62(4): 281-289.

McCartney, J. S. & Khosravi, A. (2013). Field Monitoring System for Suction and Temperature Profiles Under Pavements. *Journal of Performance of Constructed Facilities*, 27(6): 818–825.

Mishra, D. & Tutumluer, E. (2012). Aggregate physical properties affecting modulus and deformation characteristics of unsurfaced pavements. *Journal of Materials in Civil Engineering, ASCE*, 24(9): 1144-1152.

Ng, C. W. W. & Xu, J. (2012). Effects of current suction ratio and recent suction history on small-strain behaviour of an unsaturated soil. *Canadian Geotechnical Journal*, 49(2): 226-243.

Ng, C. W. W. & Yung, S. Y. (2008). Determination of the anisotropic shear stiffness of an unsaturated decomposed soil. *Géotechnique*, 58(1): 23-35.

Ng, C. W. W. & Zhou, C. (2014). Cyclic behaviour of an unsaturated silt at various suctions and temperatures. *Géotechnique*, 64(9): 709-720.

Ng, C. W. W., Zhou, C., Yuan, Q. & Xu, J. (2013). Resilient modulus of unsaturated subgrade soil: experimental and theoretical investigations. *Canadian Geotechnical Journal*, 50(2): 223-232.

Puppala, A. J., Mohammad, L. N. & Allen, A. (1999). Permanent deformation characterization of subgrade soils from RLT test. *Journal of Materials in Civil Engineering, ASCE*, 11(4): 274-282.

Romero, E., Gens, A. & Lloret, A. (2001). Temperature effects on the hydraulic behaviour of an unsaturated clay. *Geotechnical & Geological Engineering*, 19(3-4): 311-332.

Romero, E., Gens, A. & Lloret, A. (2003). Suction effects on a compacted clay under non-isothermal conditions. *Géotechnique*, 53(1): 65-81.

Sivakumar, V. (1993). A critical state framework for unsaturated soil.Phd thesis, University of Sheffield.

Sivakumar, V., Kodikara, J., O'Hagan, R., Hughes, D., Cairns, P. & Mckinley, J. D. (2013). Effects of confining pressure and water content on performance of unsaturated compacted clay under repeated loading. *Géotechnique*: 628-640.

Sweere, G. T. (1990). Unbound granular bases for roads. Technische Universitiet Delft.

Wheeler, S. J. & Karube, D. (1996). Constitutive modelling. *Proceedings of the First International Conference on Unsaturated Soil. Paris, 6-8 September.*

Wheeler, S. J., Sharma, R. S. & Buisson, M. S. R. (2003). Coupling of hydraulic hysteresis and stress-strain behaviour in unsaturated soils. *Géotechnique*, 53(1): 41-54.

Zhou, C., Ng, C. W. W. & Chen, R. (2014). A bounding surface plasticity model for unsaturated soil under small strains. *International Journal for Numerical and Analytical Methods in Geomechanics*, Accepted.

List of tables

List of figures

Table 1. Test program

Specimen identity	Suction path (kPa)	Thermal path (℃)	Test duration (day)
Series 1: coupled effects of temperature and suction			
W0T20	95→0	20	12
W0T40	95→0	20→40	18
W0T60	95→0	20→60	20
W30T20	95→30	20	7
W30T40	95→30	20→40	12
W30T60	95→30	20→60	13
W60T20	95→60	20	4
W60T40	95→60	20→40	17
W60T60	95→60	20→60	11
Series 2: effects of heating and cooling			
W30HC	95→30	20→60→20	19
W60HC	95→60	20→60→20	14

Table 2. Index properties of test soil (silt)

Index test	Measured value
Standard compaction tests	
Maximum dry density: (kg/m^3)	1760
Optimum water content: (%)	16.3
Grain size distribution	
Percentage of sand: (%)	24
Percentage of silt: (%)	72
Percentage of clay: (%)	4
Specific gravity	2.73
Atterberg limits (grain size < 425 μm)	
Liquid limit: (%)	43
Plastic limit: (%)	29
Plasticity index: (%)	14

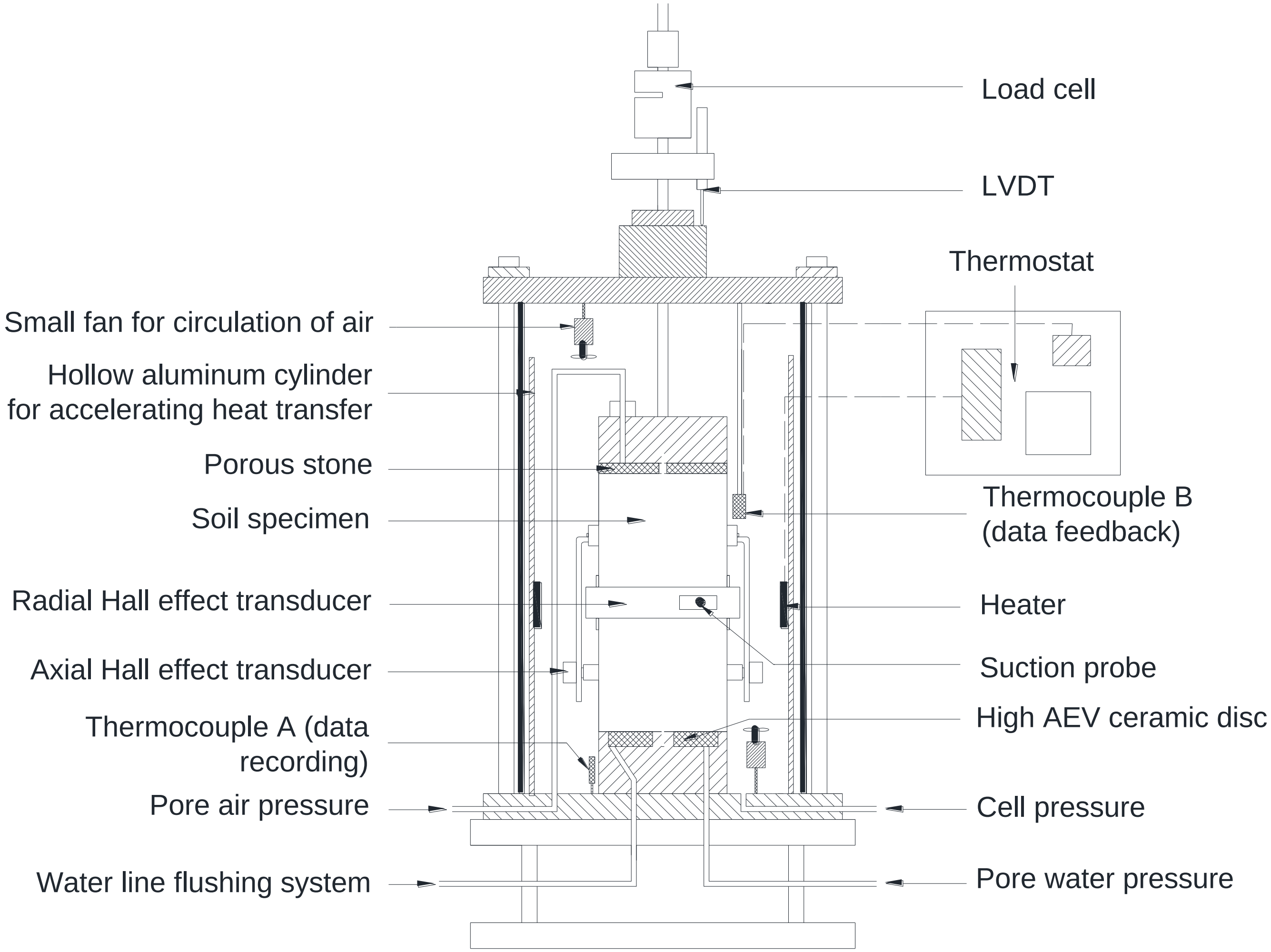

Figure 1. Temperature- and suction-controlled cyclic triaxial system (Ng and Zhou, 2014)

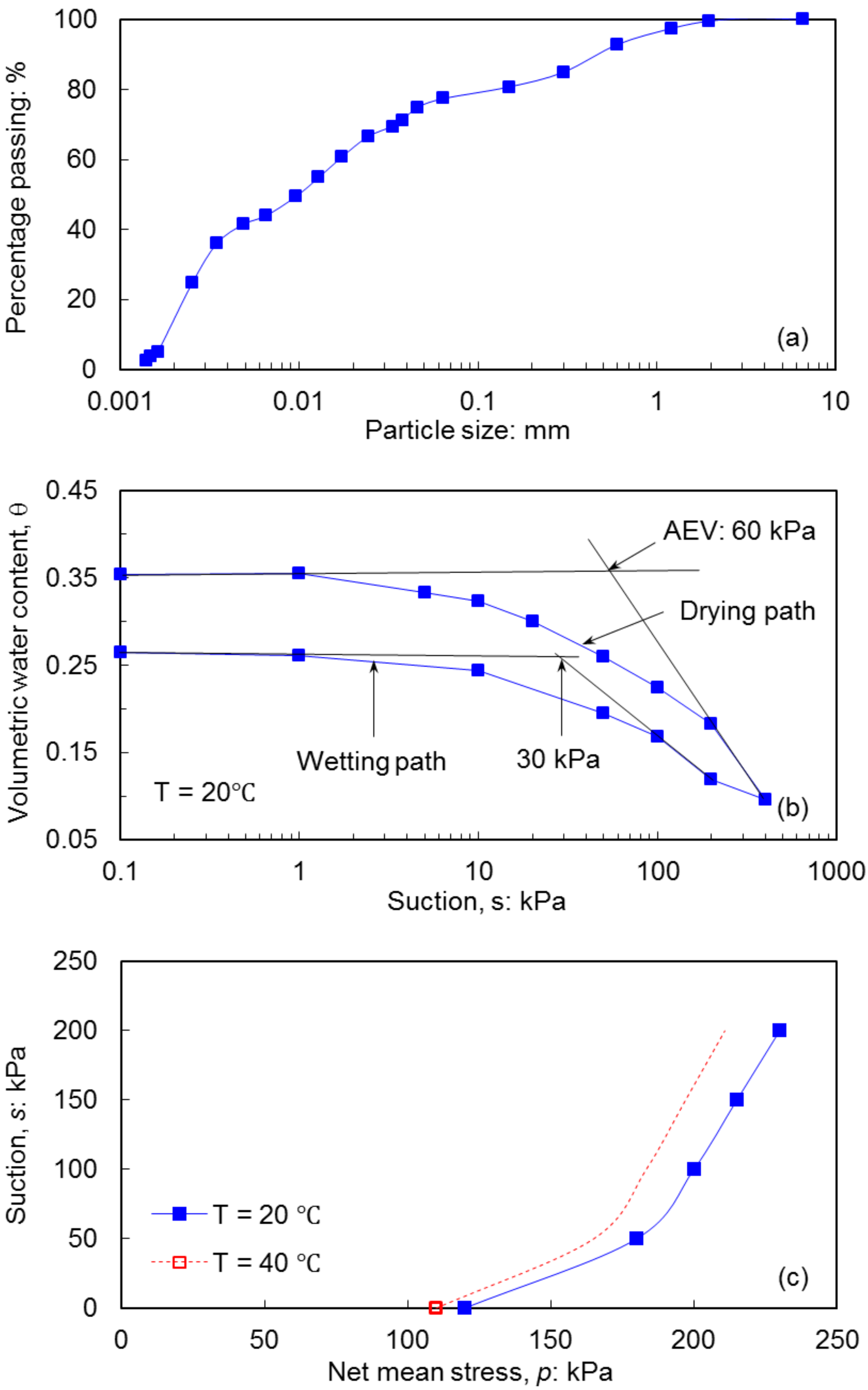

Figure 2. Properties of test soil: (a) particle size distribution; (b) water retention curve at 20℃; (c) yield stress at various suctions and temperatures

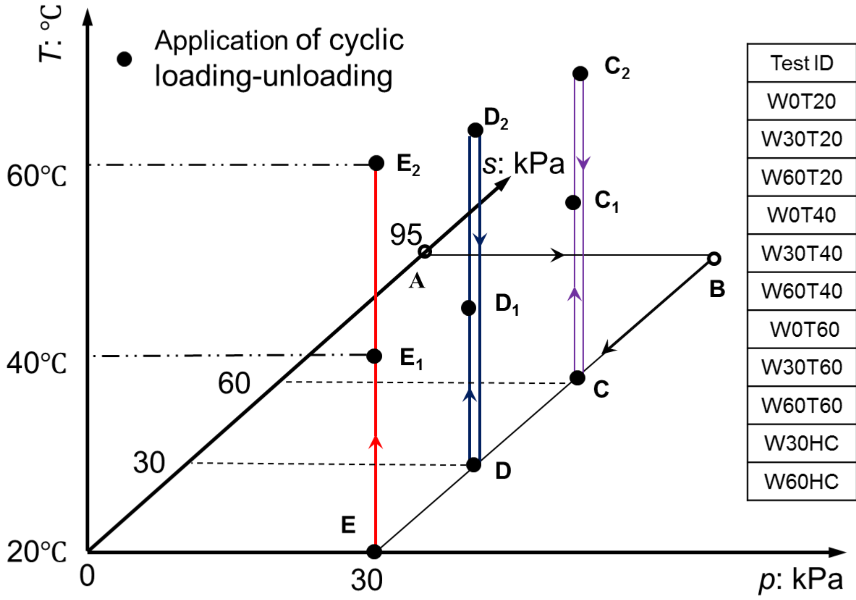

Test ID	Stress paths
W0T20	A→B→E
W30T20	A→B→D
W60T20	A→B→C
W0T40	A→B→E→E_1
W30T40	A→B→D→D_1
W60T40	A→B→C→C_1
W0T60	A→B→E→E_2
W30T60	A→B→D→D_2
W60T60	A→B→C→C_2
W30HC	A→B→D→D_2→D
W60HC	A→B→C→C_2→C

Figure 3. Stress paths for temperature- and suction-controlled cyclic triaxial tests

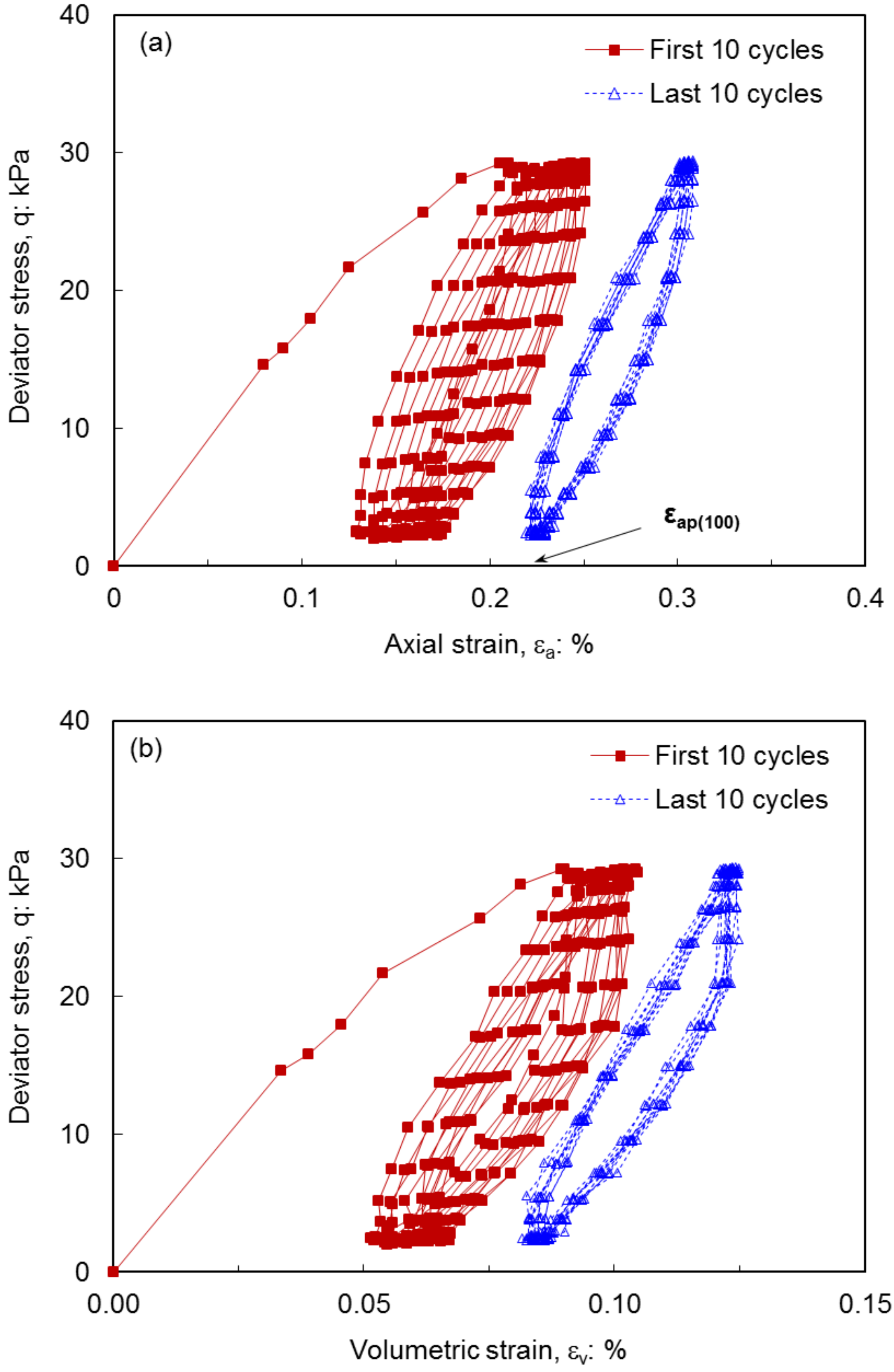

Figure 4. Soil response during a typical triaxial test (W0T20): (a) stress-strain relationship; (b) volume change

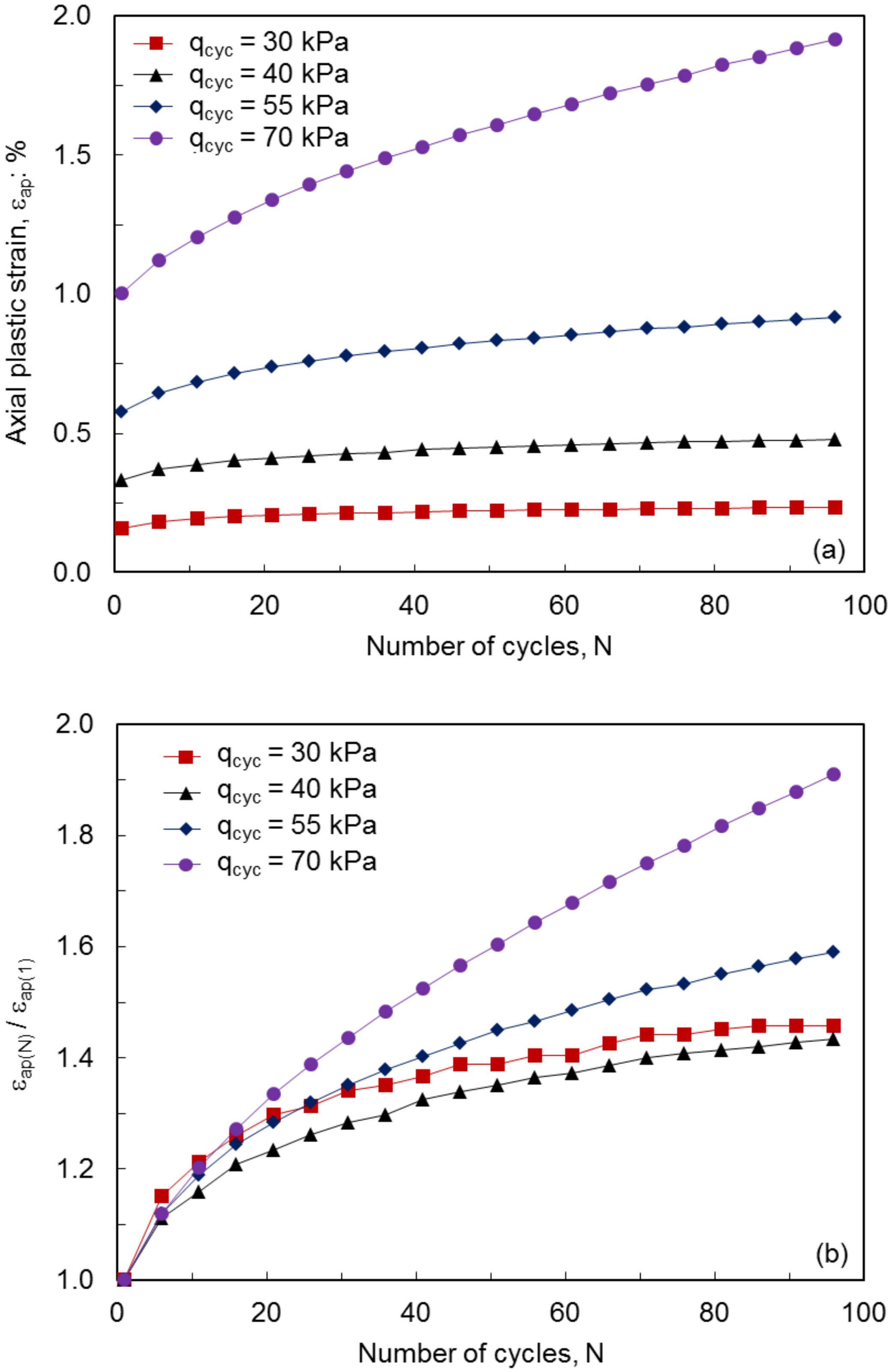

Figure 5. Influence of number of cycles on plastic strain accumulation (test W0T20): (a) plastic strain; (b) plastic strain normalized by plastic strain induced by the first cycle

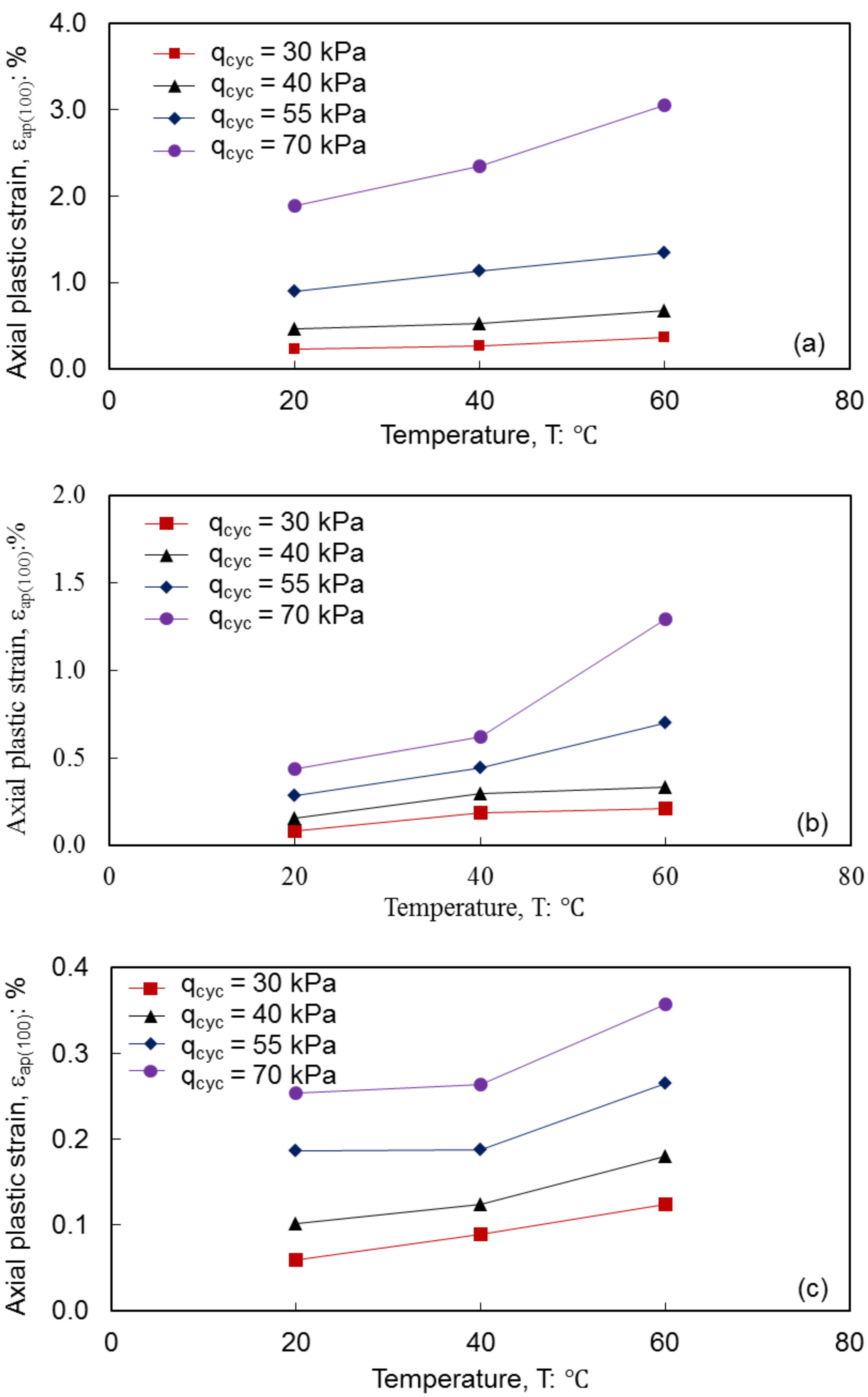

Figure 6. Influence of temperature on plastic strain accumulation at different suctions: (a) zero suction; (b) 30 kPa; (c) 60 kPa

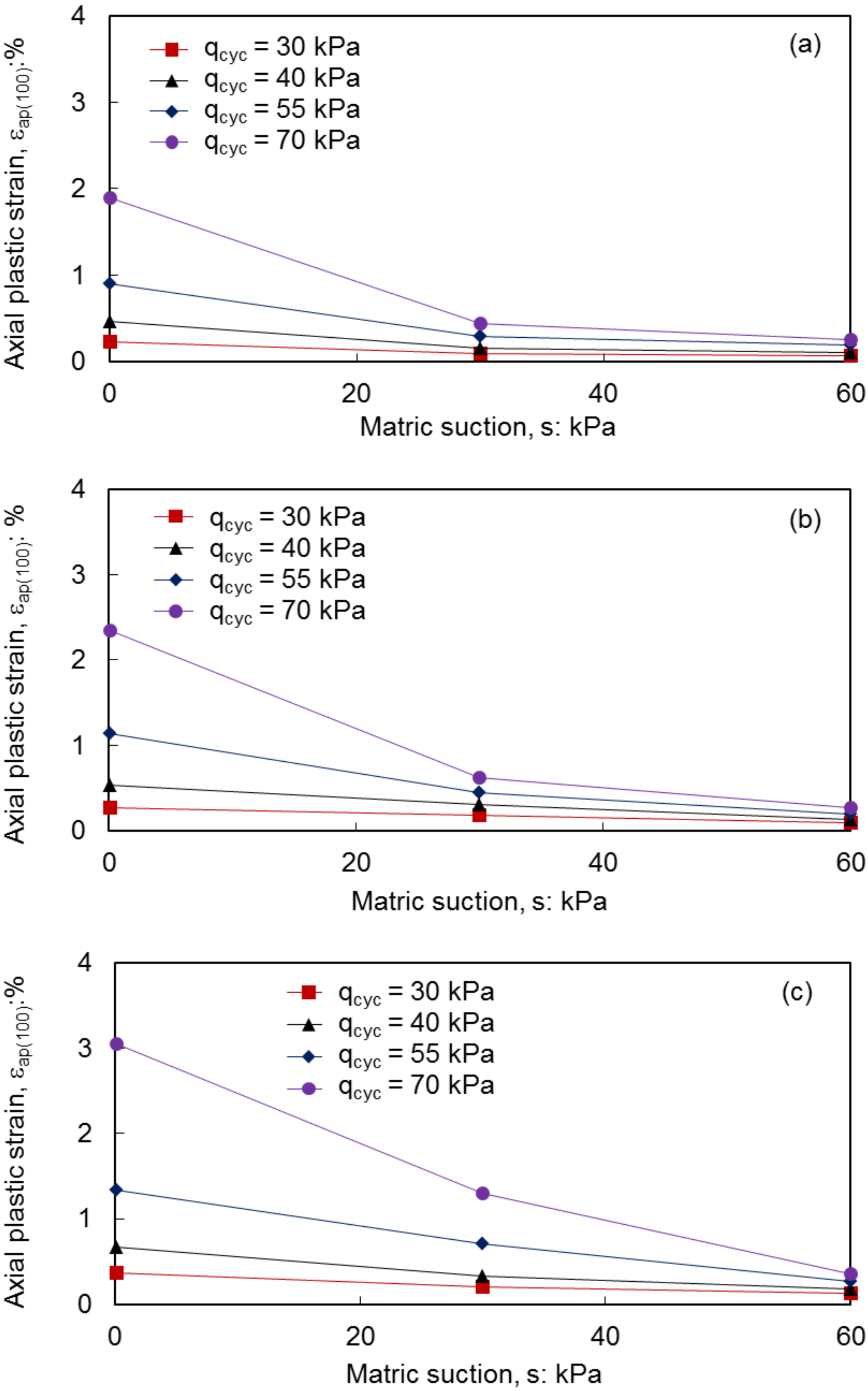

Figure 7. Influence of suction on plastic strain accumulation at different temperatures: (a) 20℃; (b) 40℃; (c) 60℃

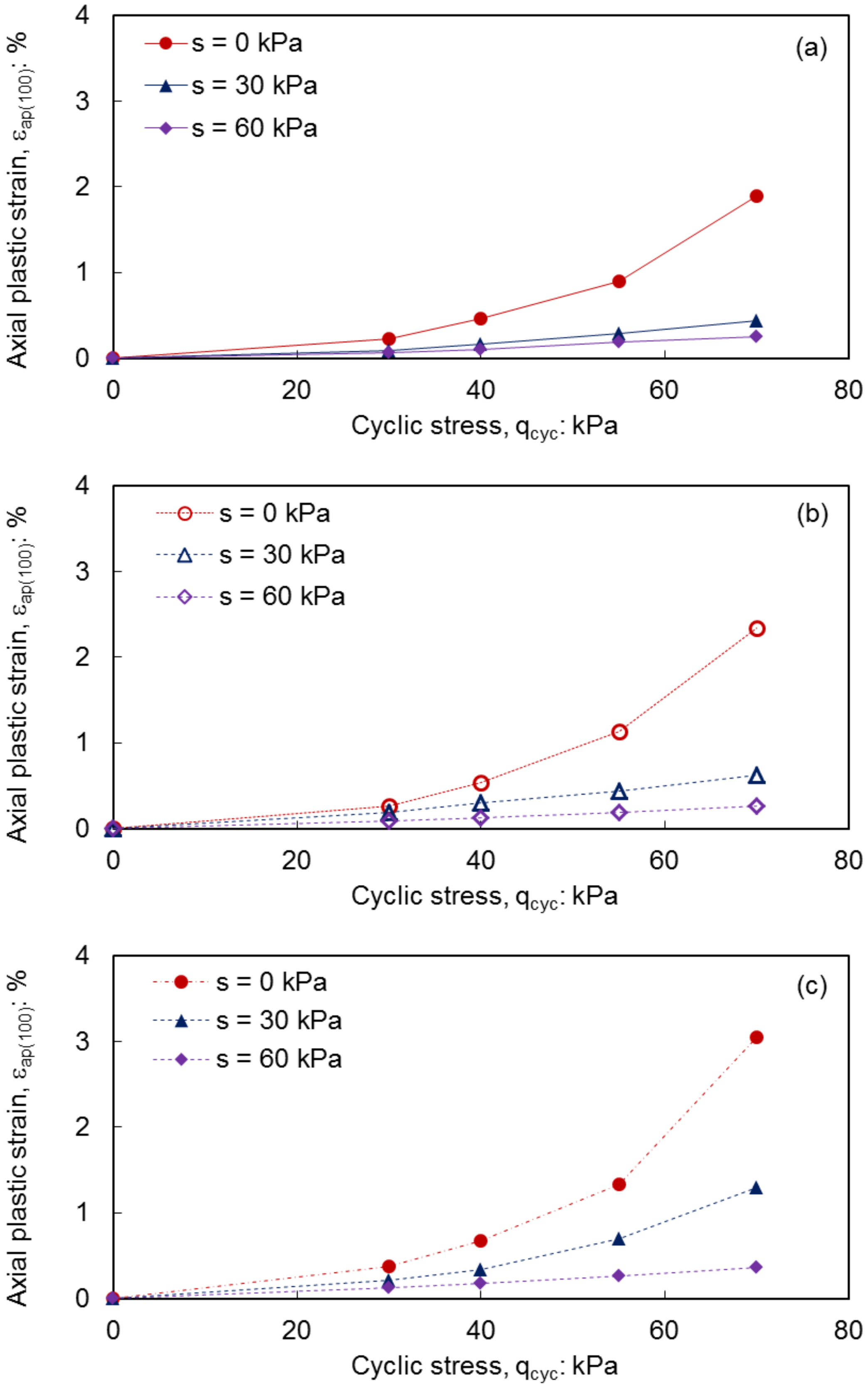

Figure 8. Influence of cyclic stress on plastic stain accumulation at different temperatures: (a) 20℃; (b) 40℃; (c) 60℃

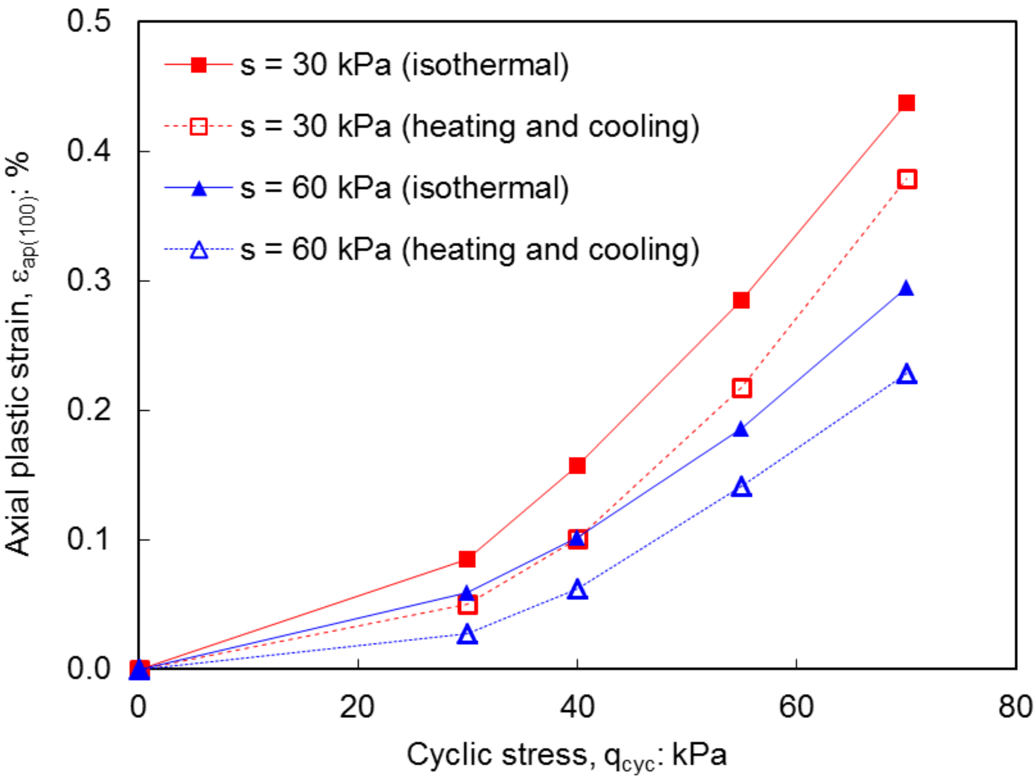

Figure 9. Influence of heating and cooling on plastic strain accumulation